Global Journal of Researches in Engineering: F
Electrical and Electronics Engineering
Volume 18 Issue 1 Version 1.0 Year 2018
Type: Double Blind Peer Reviewed International Research Journal
Publisher: Global Journals
Online ISSN: 2249-4596 & Print ISSN: 0975-5861

Transient Stability Enhancement of DFIG based Wind Generator by Switching Frequency Control Strategy with Parallel Resonance Fault Current Limiter

By M. R. Islam & M. R. I. Sheikh
Rajshahi University of Engineering & Technology

Abstract- Doubly fed induction generator (DFIG) based wind turbine generation system is generally sensitive to the grid faults as its stator windings are directly connected to the grid. As the wind power penetration to the grid increases day by day, a complete shutdown of a large wind farm is not supported and continuity of power supply during grid faults according to the grid codes is very important. So, it is essential to improve the transient stability of DFIG based wind generation system. This paper investigates the impact of increasing the switching frequency of power converters of DFIG during fault conditions, and this switching frequency control (SFC) strategy is conjugated with parallel resonance fault current limiter (PRFCL) to enhance the fault ride through (FRT) of DFIG.

Keywords: doubly-fed induction generator (DFIG), fault ride through (FRT), bridge type fault current limiter (BFCL), parallel resonance fault current limiter (PRFCL), switching frequency control (SFC) strategy.

GJRE-F Classification: FOR Code: 290901

Strictly as per the compliance and regulations of:

Transient Stability Enhancement of DFIG based Wind Generator by Switching Frequency Control Strategy with Parallel Resonance Fault Current Limiter

M. R. Islam [α] & M. R. I. Sheikh [σ]

Abstract- Doubly fed induction generator (DFIG) based wind turbine generation system is generally sensitive to the grid faults as its stator windings are directly connected to the grid. As the wind power penetration to the grid increases day by day, a complete shutdown of a large wind farm is not supported and continuity of power supply during grid faults according to the grid codes is very important. So, it is essential to improve the transient stability of DFIG based wind generation system. This paper investigates the impact of increasing the switching frequency of power converters of DFIG during fault conditions, and this switching frequency control (SFC) strategy is conjugated with parallel resonance fault current limiter (PRFCL) to enhance the fault ride through (FRT) of DFIG. It is found that the proposed SFC strategy with PRFCL (SFC-PRFCL) is a very effective mean to augment the FRT capability. To check the effectiveness of that SFC-PRFCL, its performance is compared with the bridge type fault current limiter (BFCL)[3] and PRFCL [30]. Simulations were carried out using the PSCAD/EMTDC software. Both symmetrical and asymmetrical faults are considered here to check the transient responses.

Keywords: doubly-fed induction generator (DFIG), fault ride through (FRT), bridge type fault current limiter (BFCL), parallel resonance fault current limiter (PRFCL), switching frequency control (SFC) strategy.

I. Introduction

Public opposition is growing towards the use of fossil fuels as the conventional electricity generation ingredients because fossil fuels are responsible for emitting huge CO_2 and contributing global warming problems. Also because of the limited stock of fossil fuels, renewable energies can be the alternative. Among those renewable energies, wind energy is very fast growing, and it is expected that by 2020, almost 10% of global electricity generation will be provided by the wind energy [1].

Recently fixed speed wind turbine generation system lost its popularity mainly because it suffers various problems, particularly during the transient conditions. So, at present variable speed wind turbine generation system is more popular choice [2]. Due to variable speed operation, superior energy capture ability from wind, excellent power quality, higher efficiency, reduced losses, less mechanical stress on turbine, fractionally rated converter, separate control ability of active and reactive power make doubly fed induction generator (DFIG) one of the most popular choices in wind energy market [3, 4].

Although DFIG has many unique advantages, it suffers from grid disturbances as its stator windings are directly connected to the grid, and rotor windings are connected to the grid via back to back power electronic converters. The shutdown of that DFIG based wind farm during a fault is the easiest solution but not the wise one as more and more wind power is integrated into the grid. Therefore various grid codes [5] have been defined to avoid the complete shutdown of a large wind farm. DFIG may experiences high current in both stator and rotor windings, DC-link overvoltage, torque oscillation, acute mechanical stress to the rotor shaft and gearbox during the fault condition. So, enhance the fault ride through (FRT), or low voltage ride through (LVRT) capability of DFIG is very important.

To enhance the FRT capability of the DFIG based wind generation system, many solutions have been proposed, which can be categorized into two groups.

- Using new converter modeling and control techniques. It increases the complexity of the system.
- Using auxiliary devices, also known as hardware solutions. It increases the overall cost of the system.

In [6-12] describe some FRT solutions by using the first group. The second group uses auxiliary devices, where in [13-16] a crowbar was used to improve the FRT capability of DFIG, while in [17, 18] a DC-chopper was used. Use of series dynamic braking resistor (SDBR) and dynamic voltage restorer (DVR) were described in [19-21] and [22, 23] respectively. Static synchronous compensator (STATCOM) [24], switch type

Author α σ: Department of Eletrical & Electronic Engineering Rajshahi University of Engineering & Technology, Rajshahi-6204, Bangladesh.
e-mails: rashu_ruet@yahoo.com, ris_eee@ruet.ac.bd

fault current limiter (STFCL) [25], resistive type superconducting fault current limiter (SFCL) connected in a series with the DFIG rotor winding [26], superconducting magnetic energy storage (SMES) [27], nine-switch converter (NSC) instead of six-switch converter [28] are also proposed as a solution to improve the FRT capability of DFIG.

In previous work, it has proved that bridge type fault current limiter (BFCL) [3] is an excellent solution to enhance FRT capability of DFIG based variable speed wind generation system. As a new auxiliary device named parallel resonance fault current limiter (PRFCL) has a promising application in power systems [29]. Application of PRFCL to augment the FRT capability of DFIG based wind farm is reported in [30], and it has found from that paper that the PRFCL has better FRT augmentation capability than the BFCL. Now in this paper, the effect of increasing the switching frequency of power converters of DFIG during fault conditions is observed, and this switching frequency control (SFC) strategy is conjugated with the PRFCL (SFC-PRFCL) to augment the FRT capability of DFIG. Both symmetrical and asymmetrical faults are considered at the most vulnerable point of the system. In order to check the effectiveness of that SFC-PRFCL, its performance is compared with both the BFCL and the PRFCL. Simulation results show that SFC-PRFCL outperforms both the BFCL and the PRFCL. Simulations were carried out in PSCAD/EMTDC environment.

II. Model System

The effectiveness of the proposed SFC-PRFCL is demonstrated through a test wind energy conversion system. Here in Fig. 1, a DFIG (10 MVA) is connected to the point of common coupling (PCC). The output of the wind turbine is supplied to the utility grid through a 0.69/11-kV step-up transformer and double circuit transmission lines. The rotor of that DFIG is fed through a 0.34/0.69-kV step-down transformer and back-to-back converters named rotor side converter (RSC) and grid side converter (GSC) that use insulated gate bipolar transistors (IGBTs). A capacitor is connected to the DC side acts as the DC voltage source. The SFC- PRFCL is connected in series with one of the transmission lines to protect it. At the most vulnerable point of the system, both symmetrical and asymmetrical faults were considered.

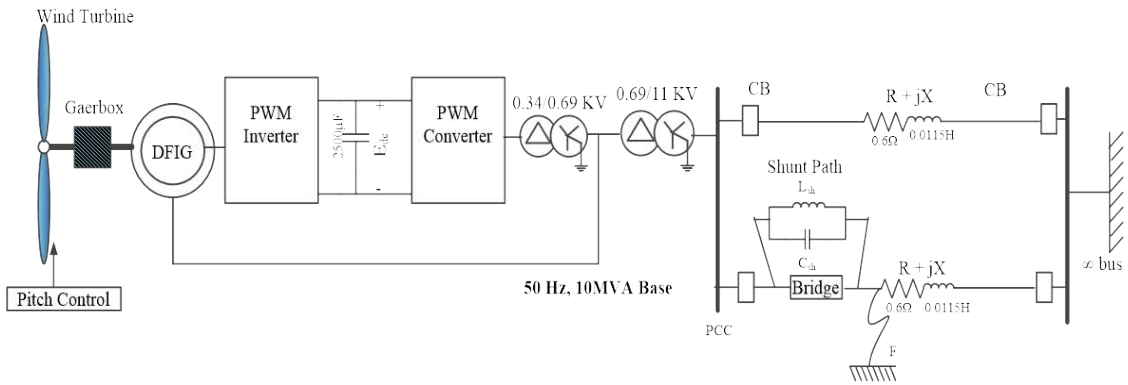

Fig. 1: Schematic diagram of the study system.

III. Wind Turbine and DFIG Modeling

Modeling of the wind turbine, the DFIG, and the converter controllers are as follows.

a) Wind Turbine Modeling

The turbine rotor, a shaft, and a gearbox unit are the primary components in the modeling of a wind turbine. Also, various physical and geometrical aspects have to take in consideration for proper modeling of a wind turbine. Normally a simplified method of modeling the wind turbine is used. The commonly used mathematical relations for the aerodynamic torque and mechanical power extracted from the wind can be given by [19]:

$$T_M = \frac{1}{2}\pi\rho C_t(\lambda) R^3 V_w^2 [NM] \quad (1)$$

$$P_{wt} = \frac{1}{2}\pi\rho C_p(\lambda,\beta) R^2 V_w^3 [W] \quad (2)$$

where ρ is the air density, R is the radius of the turbine, V_w is the wind speed, and $C_p(\lambda,\beta)$ is the power coefficient given by

$$C_p(\lambda,\beta)=\frac{1}{2}(\Gamma-0.02\beta^2-5.6)e^{-0.17\Gamma} \quad (3)$$

The relationship between C_t and C_p can be expressed as

$$C_t(\lambda)=\frac{C_p(\lambda)}{\lambda} \quad (4)$$

$$\lambda=\frac{\omega_{wt}R}{V_w} \quad (5)$$

$$\Gamma=\frac{R(3600)}{\lambda(1609)} \quad (6)$$

Here, ω_{wt} is the rotational speed of the wind turbine, λ is the tip speed ratio, and β is the blade pitch angle.

b) DFIG Modeling

Modeling of DFIG has described in many works. Here the Park's transformation model is chosen to model the DFIG. Two mass drive train model used in this study. Drive train model has a great impact on transient stability. The generator parameters and excitation parameters are given in Table I [19, 31].

Table 1: Generator and excitation parameters

Characteristic	Value
Rated power	10 [MVA]
Rated voltage	0.69[kV]
Rated frequency	50[Hz]
Stator resistance	0.01[pu]
Wound rotor resistance	0.01[pu]
Magnetizing inductance	3.5[pu]
Stator leakage inductance	0.15[pu]
Wound rotor leakage inductance	0.15[pu]
Generator inertia constant	0.3 [pu]
Turbine inertia constant	3.0 [pu]
Shaft stiffness between two masses	90 [pu]
DC-link voltage	0.7 [kV]
DC-link capacitor	25,000 [μF]
Device for the power converter	IGBT

c) RSC Controller

Fig. 2 shows the RSC controller which is actually a two level, six pulse, IGBT based power converter in this study. It regulates the terminal voltage to 1.0 pu. The active power and reactive power are controlled by d-axis current and q-axis current respectively. The Park's transformation is used to convert abc-to-dq0 and vice versa. Phase lock loop (PLL) provides the angle θ_{PLL} and θ_r is the effective angle for that transformation. After getting V_{dr} and V_{qr}, those are through the dq0-to-abc transformation to produce three phase reference signal, then sent to pulse width modulation (PWM) signal generator block, so that it can generate pulses for the IGBT switches of the RSC.

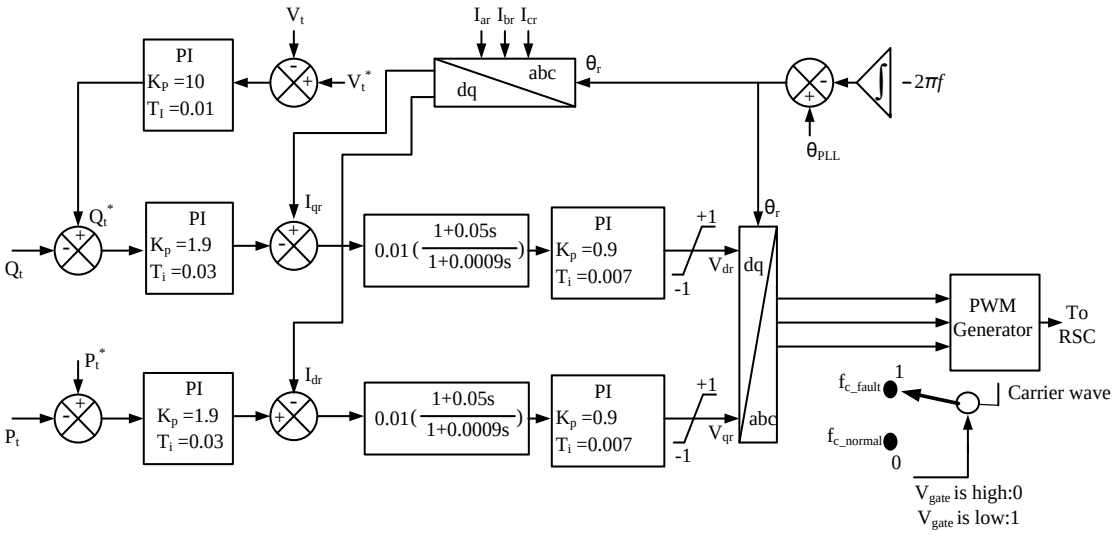

Fig. 2: RSC Controller.

d) GSC Controller

Fig. 3 shows the GSC control block for this study which also contains two level, six pulse, IGBT based power converter. It controls the DC-link voltage to 1.0 pu. The DC-link voltage and the reactive power of GSC are controlled by d-axis current and q-axis current respectively. As an odd multiple of the third harmonics, a switching frequency of 1650 Hz is chosen in the normal condition which can minimize up to thirteenth harmonics [3].

In Fig. 2 and 3, quantities with '*' refer to reference value. Parameters of proportional integral (PI) are so chosen that they can give the optimum performance. Transfer functions are used in the controllers, and their parameters are also so chosen that they give faster response and take a shorter time to reach the normal operation.

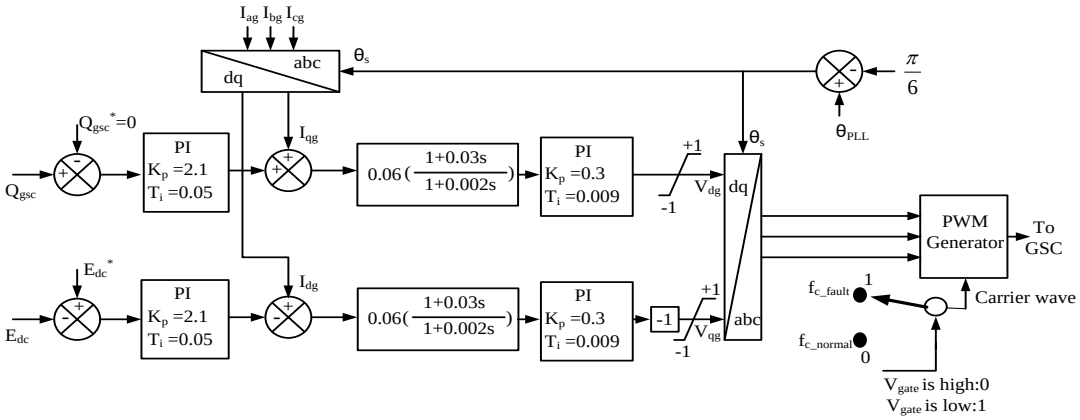

Fig. 3: GSC Controller.

IV. SFC-PRFCL

The modeling of the proposed SFC-PRFCL is described as follows.

a) PRFCL Configuration

Fig. 4 shows the per phase diagram of PRFCL [29]. It has two independent parts, namely the bridge part and the shunt part. This shunt part can be named as resonance part also.

Four diodes $D_1 - D_4$ are there in the bridge part, which are arranged in a bridge configuration. Inside the bridge, a small valued DC reactor L_{dc} in series with an IGBT switch is placed as shown in Fig. 4. For safety purpose, a free-wheeling diode D_5 is equipped with the

DC reactor L_{dc}. A very small value resistor R_{dc} is considered in series with L_{dc} to include the latent resistance of the DC reactor.

The shunt or resonance part is constructed of a capacitor C_{sh} and an inductor L_{sh}. To form an LC resonance circuit at line power frequency, they are arranged in parallel to each other as shown in Fig. 4.

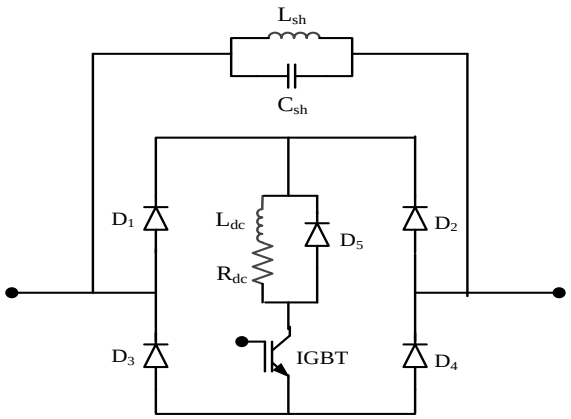

Fig. 4: Per phase PRFCL configuration.

b) PRFCL Operation and Control

In normal operating condition, the IGBT switch in Fig. 4 is in ON state. In the positive half cycle, the $D_1 - L_{dc} - R_{dc} - D_4$ path and in the negative half cycle, the $D_2 - L_{dc} - R_{dc} - D_3$ path carries the line current. So, the current through the DC reactor L_{dc} is in the same direction, and this is the DC current i_{dc} for L_{dc}. This L_{dc} offers no impedance for this DC current. There are some voltage drop in the bridge part during normal operating condition due to the latent resistance R_{dc} of the DC reactor, ON-state resistance of IGBT switch and diode forward voltage drop. But the aggregated voltage drop of those is ignorable compared to the large line voltage drop. So, this bridge part has no impact on normal operating condition. As the shunt path is in the parallel resonance condition, its impedance seems very high. Therefore in normal condition, the full line current is flown through the bridge part except some negligible leakage current.

Now, when a fault occurs, the line current wants to rise very quickly, but the DC reactor L_{dc} does not permit this. So, safe operation for IGBT switch is ensured as L_{dc} limits the high $^{di}/_{dt}$ value during fault. To take the turn OFF decision for IGBT switch during a fault and bypass the line current to the high impedance resonating shunt path, DC current i_{dc} through the DC reactor is compared with a threshold value i_{th}. Here, i_{th} is taken 1.3 times the nominal value of i_{dc} for optimum operation. When i_{dc} exceeds i_{th}, IGBT switch gets a low gate signal V_{gate} and turned OFF. Per phase PRFCL controller is shown in Fig.5. Some other parameters like the line current, the terminal voltage, the active power or the reactive power can be used for IGBT control, but the DC current i_{dc} through the DC reactor L_{dc} is used in this study. This is because i_{dc} is very sensitive to line current and has a faster rate of rise than line current and other parameters.

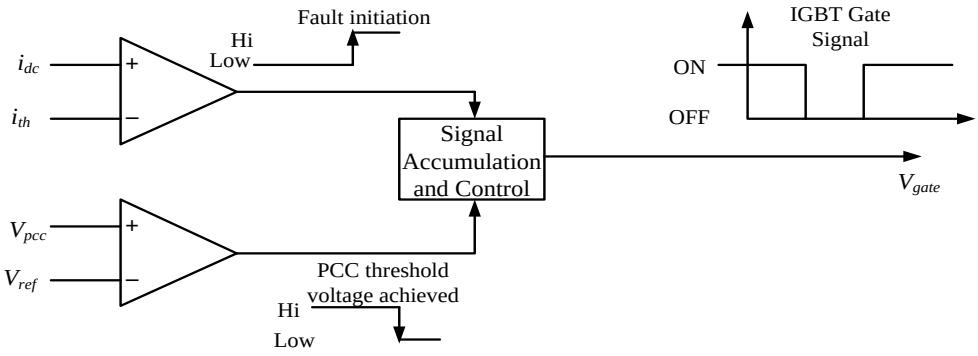

Fig. 5: Per phase controller for PRFCL.

After turning OFF of the IGBT, i_{dc} becomes zero. So, to resume the normal operation and turn ON the IGBT switch, another parameter has to choose. For that purpose, the voltage at PCC, V_{PCC} is chosen in this study. After the circuit breakers opening of the faulty section and isolating that faulty part, bus voltage starts to rise, and the system starts to recover. The V_{PCC} is compared with a reference value V_{ref} which is set 90% of the nominal value of V_{PCC}. After starting the rise of bus voltage, when V_{PCC} exceeds V_{ref}, the IGBT switch will get a high signal and normal operation resume as shown in Fig. 5.

c) PRFCL Design Consideration

To design the PRFCL, the ultimate task is to determine the values of shunt capacitor C_{sh} and shunt inductor L_{sh}. At power frequency, so many combinations of C_{sh} and L_{sh} would give the resonance condition. Standard values of C_{sh} are picked from [32], and L_{sh} is

calculating considering the resonance at power frequency. At power frequency, many pairs of C_{sh} and L_{sh} are trialed, and among those, $C_{sh} = 125\,\mu F$ and $L_{sh} = 80\,mH$ gave the best result during the fault. The values of L_{dc} and R_{dc} are picked $1\,mH$ and $0.3m\Omega$ respectively, which give a time constant of 3.33 s. This is good enough for smoothing the DC reactor current.

d) SFC Configuration

To investigate the impact of increasing the switching frequency of the carrier wave during the fault condition, the proposed pulse generation system for both RSC and GSC is shown in Fig. 6. In both RSC and GSC, the triangular signal is used as the carrier wave of PWM operation. In Fig. 6, f_{c_nornal} is the switching frequency in normal operating condition, and f_{c_fault} is the increased switching frequency during the fault. How long the increased switching frequency f_{c_fault} will remain active is decided by the IGBT gate signal V_{gate}. As long as V_{gate} in Fig. 5 remains a low state that means the IGBT switch in Fig. 4 is in OFF state, which indicates the fault situation, f_{c_fault} is activated. Otherwise, in normal operating condition and after resuming the normal condition after the fault, f_{c_nornal} is activated. A frequency of 1650 Hz is chosen as f_{c_nornal}. And the increased switching frequency f_{c_fault} is chosen eight times of f_{c_nornal} in this study, which is implementable. This SFC strategy with PRFCL forms the SFC-PRFCL.

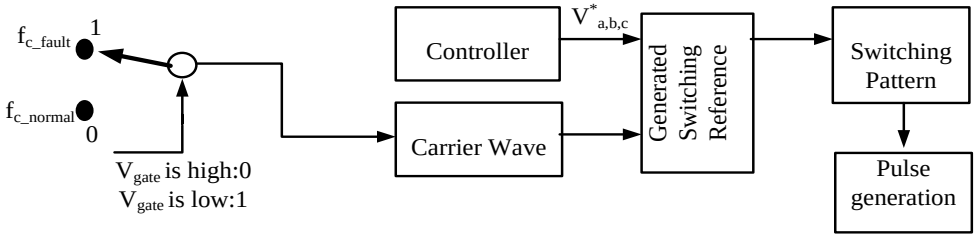

Fig. 6: Pulse generation system for both RSC and GSC (SFC strategy).

V. BFCL

To observe the effectiveness of the proposed SFC-PRFCL, its performance is compared with that the BFCL. Just like the PRFCL, the BFCL has two distinct parts namely the bridge part and the shunt path as shown in Fig. 7. Bridge part is exactly the same as PRFCL and the shunt path composed of a resistor R_{sh} in series with an inductor L_{sh}. The detail of BFCL topology is discussed in [3]. The same operation and control strategy is used for BFCL as PRFCL. The same controller is used for BFCL as shown in Fig. 5. The values of R_{sh} and L_{sh} are taken as the same procedure discussed in [3].

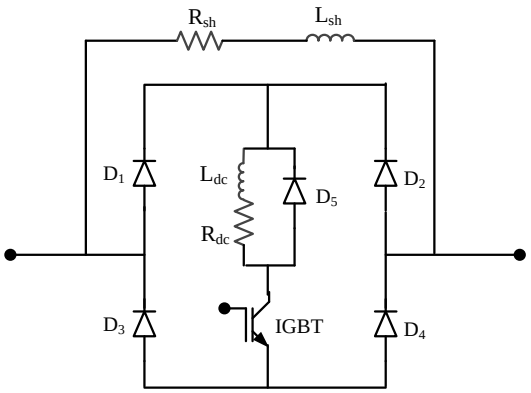

Fig. 7: Per phase BFCL configuration.

VI. Simulation Results and Discussion

Detail simulation results are described in the following subsections.

a) Simulation Considerations

Simulations were carried out by using PSCAD/EMTDC software. Here for transient analysis, a fixed wind speed of 15 m/s is considered. Duration of fault is too short to make any impact on wind speed, so fixed speed is considered. Analysis is carried out, and results are shown for most severe three line to ground (3LG) and most common line to ground (1LG) faults. Those faults were applied at the most vulnerable point of the system near the PCC denoted by point F in Fig. 1. Those faults were applied at 0.1 s and withdrawn at 0.6 s. Circuit breakers on the faulted line open and reclose at 0.2 s and 1.1 s respectively. Results are shown for a time duration of 0 s to 3 s, and per unit (pu) measurements are used. All those figures have a zoomed portion for better visualization.

b) FRT Improvement by SFC-PRFCL for 3LG fault

Fault responses for 3LG fault are shown in Figs. 8-11. Fig. 8 shows the terminal voltage profile for DFIG. With no controller, terminal voltage goes nearly zero just after the fault occurrence and continues the same way till the breakers opening. After the breaker opening, terminal voltage rises beyond 1.2 times the nominal value and takes much time to come back the pre-fault

value. The BFCL has good voltage response as compared to no controller case, but PRFCL gives a better voltage profile than the BFCL. But among those all, SFC-PRFCL has the best voltage profile with least amount of voltage fluctuation.

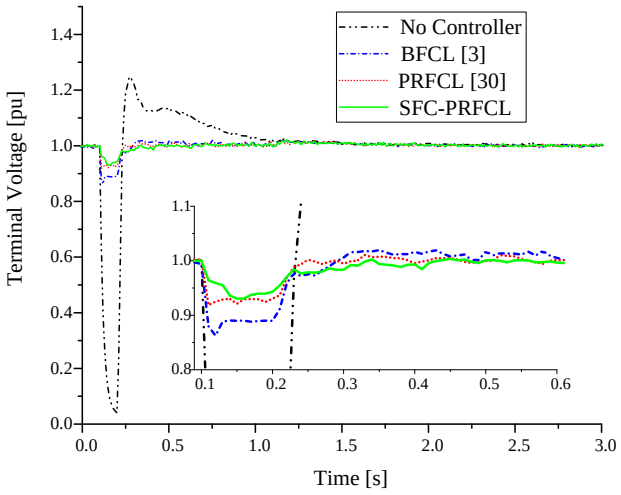

Fig. 8: Terminal voltage response for 3LG fault.

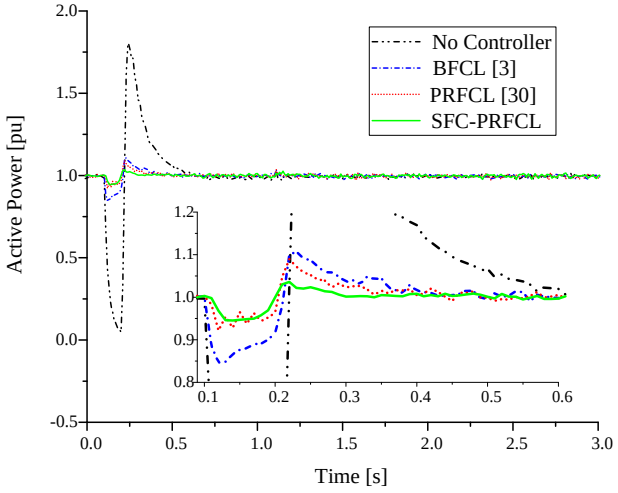

Fig. 9: Active power response for 3LG fault.

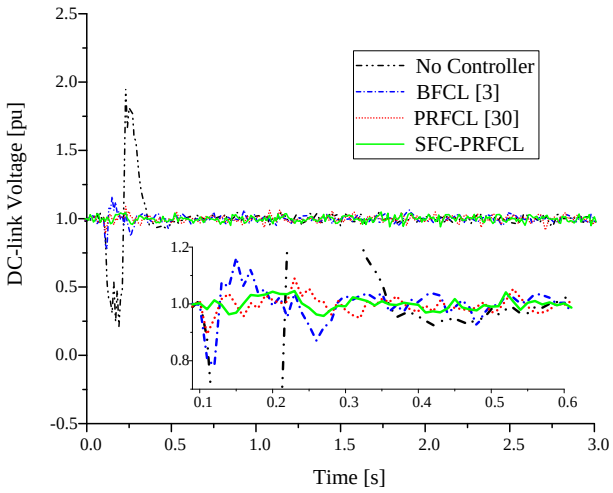

Fig. 10: DC-link voltage response for 3LG fault.

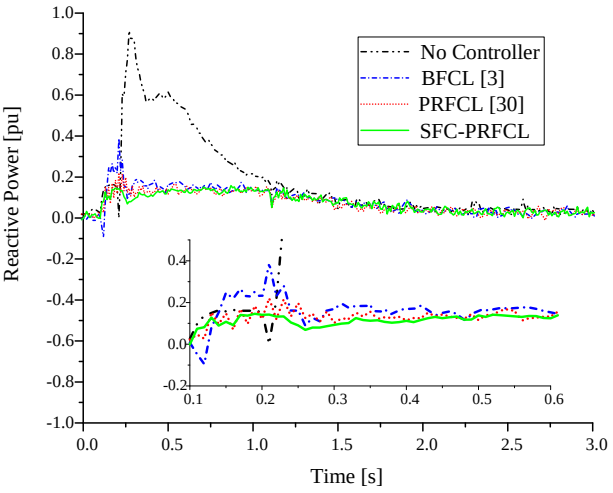

Fig. 11: Reactive power response for 3LG fault.

It is clear from the Fig. 9 that the SFC-PRFCL keeps the active power profile smooth during a 3LG fault. Output power goes very close to zero after the fault event with no controller case. Also, the breakers opening causes a large imbalance of output power. The BFCL and the PRFCL both have better active power profile than no controller case, but SFC-PRFCL gives the best response.

The DFIG DC-link voltage profile is shown in Fig. 10 for 3LG fault. With no controller case, DC-link voltage profile is not good during the 3LG fault. It is seen that the DC-link voltage profile can be controlled within permissible limit by BFCL, PRFCL, and SFC-PRFCL. Among those, SFC-PRFCL gives the best DC-link voltage profile with least deviation of DC-link voltage from the nominal value.

Fig. 11 provides the reactive power profile of DFIG. It is illustrated from this figure that, BFCL and PRFCL can contribute to keep better reactive power profile, but SFC-PRFCL has superior performance than both of them.

c) *FRT Improvement by SFC-PRFCL for 1LG fault*

Fault responses for 1LG fault are shown in Figs. 12-15. Fig. 12 and Fig. 13 represent the terminal voltage profile and output active power profile respectively. It is clear from those figures that, BFCL and PRFCL have better terminal voltage and active power profiles than no controller case, but their performances are inferior to the SFC-PRFCL.

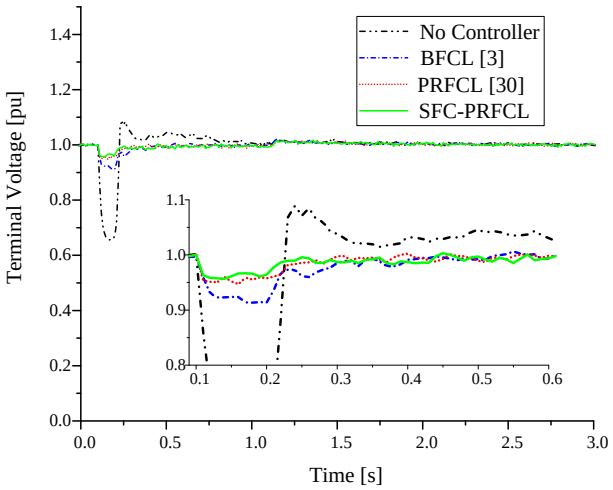

Fig. 12: Terminal voltage response for 1LG fault.

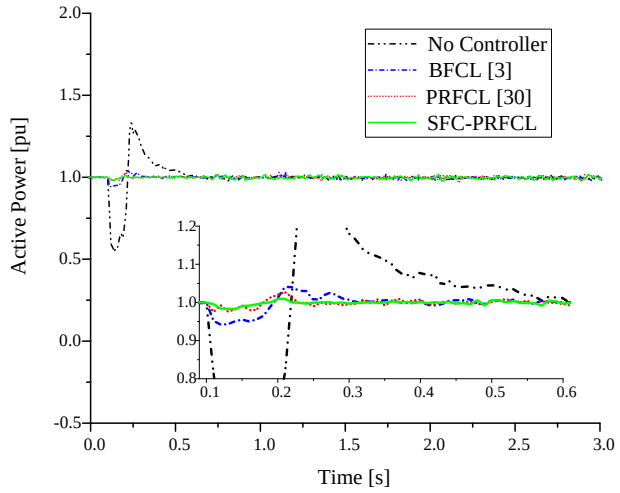

Fig. 13: Active power response for 1LG fault.

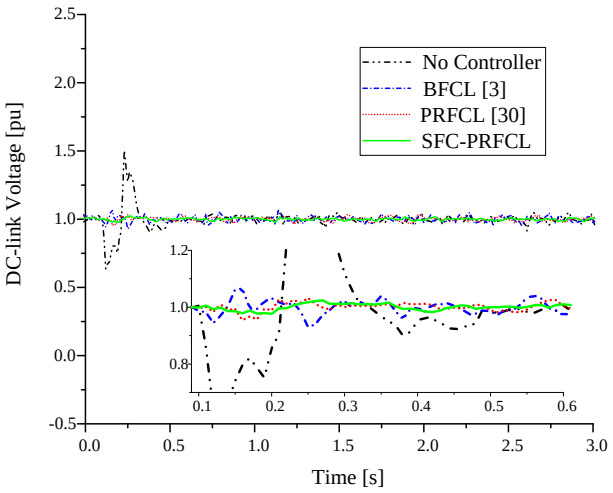

Fig. 14: DC-link voltage response for 1LG fault.

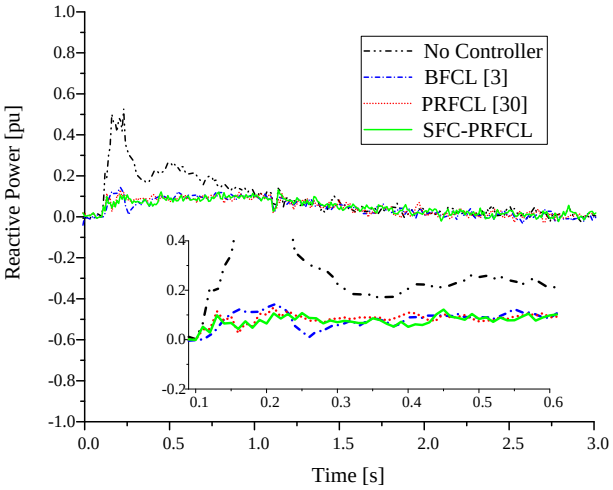

Fig. 15: Reactive power response for 1LG fault.

The DFIG DC-link voltage profile and reactive power profile are shown in Fig. 14 and Fig. 15 respectively for 1LG fault. It is apparent that the more stable operation is obtained when SFC-PRFCL is used. Figs. 8-15 indicate that the system is less affected by 1LG fault than the 3LG fault.

VII. Conclusion

The application of the SFC-PRFCL to enhance the FRT capability of DFIG is proposed in this paper. The effectiveness of the SFC-PRFCL is compared with that of the BFCL [3] and the PRFCL [30]. Following points are mentionable from the simulation results and discussions.

- The SFC-PRFCL is a very effective means to enhance the FRT capability of DFIG-based wind

turbine generation system for both symmetrical and asymmetrical faults.

- The proposed SFC-PRFCL ensures more stable operation of the DFIG-based wind turbine generation system.
- Performances of BFCL and PRFCL are outperformed by the SFC-PRFCL in every aspect.

In our future work, the usefulness of SFC-PRFCL on a high capacity DFIG-based wind farm connected to a multi-machine power system will be considered.

References Références Referencias

1. P. Musgrove, *Wind Power*. New York: Cambridge Univ. Press, 2010, pp. 221–222.
2. S. M. Muyeen, R. Takahashi, T. Murata and J. Tamura, "A Variable Speed Wind Turbine Control Strategy to Meet Wind Farm Grid Code Requirements," *IEEE Trans. Power Syst.*, vol. 25, pp. 331-340, Feb. 2010.
3. G. Rashid and M. Ali, "Transient stability enhancement of doubly fed induction machine-based wind generator by bridge-type fault current limiter," *IEEE Trans. Energy Convers.* , vol. 30, pp. 939- 947, Sept. 2015.
4. Sajjad Tohidi, Mohammadi-ivatloo Behnam, "A comprehensive review of low voltage ride through of doubly fed induction wind generators", *Renewable and Sustainable Energy Reviews*, Volume 57, Pages 412-419, May 2016.
5. M. Tsili and S. Papathanassiou, "A review of grid code technical requirements for wind farms," *IET Renew. Power Gener. ,* vol. 3, no. 3, pp. 308- 332, Sept. 2009.
6. Bo Yang, Lin Jiang, Lei Wang, Wei Yao, Q.H. Wu, "Nonlinear maximum power point tracking control and modal analysis of DFIG based wind turbine", *International Journal of Electrical Power & Energy Systems*, Volume 74, Pages 429-436,January 2016.
7. G. Kenne, J. d. D. Nguimfack Ndongmo, R. Fochie Kuate and H. B. Fotsin, "An Online Simplified Nonlinear Controller for Transient Stabilization Enhancement of DFIG in Multi-Machine Power Systems," in *IEEE Transactions on Automatic Control*, vol. 60, no. 9, pp. 2464-2469, Sept. 2015.
8. T. D. Vrionis, X. I. Koutiva and N. A. Vovos, "A Genetic Algorithm-Based Low Voltage Ride-Through Control Strategy for Grid Connected Doubly Fed Induction Wind Generators," in *IEEE Transactions on Power Systems*, vol. 29, no. 3, pp. 1325-1334, May 2014.
9. Q. Huang, X. Zou, D. Zhu and Y. Kang, "Scaled Current Tracking Control for Doubly Fed Induction Generator to Ride-Through Serious Grid Faults," in *IEEE Transactions on Power Electronics*, vol. 31, no. 3, pp. 2150-2165, March 2016.
10. Bhinal Mehta, Praghnesh Bhatt, Vivek Pandya, "Small signal stability enhancement of DFIG based wind power system using optimized controllers parameters", *International Journal of Electrical Power & Energy Systems*, Volume 70, Pages 70-82, September 2015.
11. Y. Liu, Q. H. Wu and X. X. Zhou, "Co-Ordinated Multiloop Switching Control of DFIG for Resilience Enhancement of Wind Power Penetrated Power Systems," in *IEEE Transactions on Sustainable Energy*, vol. 7, no. 3, pp. 1089-1099, July 2016.
12. J. Chen, W. Zhang, B. Chen and Y. Ma, "Improved Vector Control of Brushless Doubly Fed Induction Generator under Unbalanced Grid Conditions for Offshore Wind Power Generation," in *IEEE Transactions on Energy Conversion*, vol. 31, no. 1, pp. 293-302, March 2016.
13. S. Swain and P. K. Ray, "Short circuit fault analysis in a grid connected DFIG based wind energy system with active crowbar protection circuit for ridethrough capability and power quality improvement", *Int. J. Elect. Power Energy Syst.,* vol. 84, page 64-65, Jan. 2017.
14. G. Pannell, D. J. Atkinson and B. Zahawi, "Minimum-Threshold Crowbar for a Fault-Ride-Through Grid-Code-Compliant DFIG Wind Turbine," in *IEEE Transactions on Energy Conversion*, vol. 25, no. 3, pp. 750-759, Sept. 2010.
15. J. Vidal, G. Abad, J. Arza and S. Aurtenechea, "Single-Phase DC Crowbar Topologies for Low Voltage Ride Through Fulfillment of High-Power Doubly Fed Induction Generator-Based Wind Turbines," in *IEEE Transactions on Energy Conversion*, vol. 28, no. 3, pp. 768-781, Sept. 2013.
16. S. Swain and P. K. Ray, "Fault ridethrough and power quality improvement of Doubly-Fed Induction Generator based wind turbine system during grid fault with Novel Active Crowbar Protection design," *IEEE Region 10 Conference (TENCON)*, Singapore, 2016, pp. 2628-2633.
17. G. Pannell, B. Zahawi, D. J. Atkinson and P. Missailidis, "Evaluation of the Performance of a DC-Link Brake Chopper as a DFIG Low-Voltage Fault-Ride-Through Device," in *IEEE Transactions on Energy Conversion*, vol. 28, no. 3, pp. 535-542, Sept. 2013.
18. A. Jalilian, S. B. Naderi, M. Negnevitsky, M. T. Hagh and K. M. Muttaqi, "Controllable DC-link fault current limiter augmentation with DC chopper to improve fault ride-through of DFIG," *IET Renew. Power Gener.* vol. 11, pp. 313-324, Feb. 2017.

19. K. E. Okedu, S. M. Muyeen, R. Takahashi and J. Tamura, "Wind Farms Fault Ride Through Using DFIG With New Protection Scheme," in *IEEE Transactions on Sustainable Energy*, vol. 3, no. 2, pp. 242-254, April 2012.
20. J. Yang, J. E. Fletcher and J. O'Reilly, "A Series-Dynamic-Resistor-Based Converter Protection Scheme for Doubly-Fed Induction Generator During Various Fault Conditions," in *IEEE Transactions on Energy Conversion*, vol. 25, no. 2, pp. 422-432, June 2010.
21. A. Causebrook, D. J. Atkinson, and A. G. Jack, "Fault ride-through of large wind farms using series dynamic braking resistors," *IEEE Trans. Power Syst.*, vol. 22, no. 3, pp. 966–975, Aug. 2007.
22. B. Wessels, F. Gebhardt and F. W. Fuchs, "Fault Ride-Through of a DFIG Wind Turbine Using a Dynamic Voltage Restorer During Symmetrical and Asymmetrical Grid Faults," in *IEEE Transactions on Power Electronics*, vol. 26, no. 3, pp. 807-815, March 2011.
23. C. O. Ibrahim, T. H. Nguyen, D. C. Lee and S. C. Kim, "A Fault Ride-Through Technique of DFIG Wind Turbine Systems Using Dynamic Voltage Restorers," in *IEEE Transactions on Energy Conversion*, vol. 26, no. 3, pp. 871-882, Sept. 2011.
24. D.V.N. Ananth, G.V. Nagesh Kumar, "Fault ride-through enhancement using an enhanced field oriented control technique for converters of grid connected DFIG and STATCOM for different types of faults", *ISA Transactions*, Volume 62, Pages 2-18, May 2016.
25. W. Guo, L. Xiao, S. Dai, Y. Li, X. Xu, W. Zhou and L. Li, "LVRT capability enhancement of DFIG with switch type fault current limiter " *IEEE Trans. Ind. Electron.*, vol. 62, pp. 332-342, Jan. 2015.
26. Z. C. Zou, X. Y. Xiao, Y. F. Liu, Y. Zhang and Y. H. Wang, "Integrated Protection of DFIG-Based Wind Turbine With a Resistive-Type SFCL Under Symmetrical and Asymmetrical Faults," in *IEEE Transactions on Applied Superconductivity*, vol. 26, no. 7, pp. 1-5, Oct. 2016.
27. A. M. S. Yunus, M. A. S. Masoum and A. Abu-Siada, "Application of SMES to Enhance the Dynamic Performance of DFIG During Voltage Sag and Swell," in *IEEE Transactions on Applied Superconductivity*, vol. 22, no. 4, Aug. 2012.
28. G. Wen, Y. Chen, Z. Zhong and Y. Kang, "Dynamic Voltage and Current Assignment Strategies of Nine-Switch-Converter-Based DFIG Wind Power System for Low-Voltage Ride-Through (LVRT) Under Symmetrical Grid Voltage Dip," in *IEEE Transactions on Industry Applications*, vol. 52, no. 4, pp. 3422-3434, July-Aug. 2016.
29. S. B. Naderi, M. Jafari and M. Tarafdar Hagh, "Parallel-Resonance-Type Fault Current Limiter," in *IEEE Transactions on Industrial Electronics*, vol. 60, no. 7, pp. 2538-2546, July 2013.
30. G. Rashid and M. H. Ali, "Application of parallel resonance fault current limiter for fault ride through capability augmentation of DFIG based wind farm," in *Proc. IEEE/PES Transmission and Distribution (T&D) Conference and Exposition*, Dallas, TX, May 2016, pp. 1-5.
31. M. R. Islam, M. R. I. Sheikh and Z. Tasneem, "A frequency converter control strategy of DFIG based wind turbine to meet grid code requirements," in *Proc. 2nd IEEE International Conference on Electrical, Computer & Telecommunication Engineering (ICECTE)*, Rajshahi, Dec. 2016, pp. 1-4.
32. General Atomics Electronics Systems, "High voltage capacitors and power supplies." [Online]. Available: http://www.ga.com/capacitors. (Date accessed: 15 Aug. 2017).